

APPROPRIATE REALISATION OF GAIN-SCHEDULED CONTROLLERS WITH APPLICATION TO WIND TURBINE REGULATION

D.J.Leith
W.E.Leithead

Department of Electronic & Electrical Engineering,
University of Strathclyde,
GLASGOW G1 1QE, U.K.

Abstract

Power regulation of horizontal-axis grid-connected up-wind constant-speed pitch-regulated wind turbines presents a demanding control problem with the plant, actuation system and control objectives all strongly nonlinear. In this paper, a novel nonlinear control strategy is devised which, in some sense, optimises performance across the operating envelope. In comparison with linear control, the nonlinear strategy achieves a substantial improvement in performance. The realisation adopted is crucial in attaining the required performance. An extended local linear equivalence condition is introduced which provides a basis for the selection of an appropriate realisation. This is an important, and general, issue in the design of gain-scheduled systems and generic realisations, which satisfy the extended local linear equivalence condition, are derived for SISO systems scheduled upon an internal plant or controller variable. For the wind turbine nonlinear controller, realisations which satisfy the extended local linear equivalence condition provide a substantial improvement in performance in comparison to linear control and realisations which do not satisfy this condition.

1. Introduction

Wind energy is one of the most promising sources of renewable energy for the U.K and over the last two decades there has been rapid development of wind turbine technology. The standard commercial design of turbine is a horizontal-axis grid-connected up-wind medium-scale machine with a rating of approximately 300 kW to 500 kW. It is anticipated that the next generation of wind turbines which are presently being developed will include large-scale designs with a rating of around 1 MW. The rotor usually has two or three blades and in pitch regulated machines the pitch angle of either the full span of the blades, or just the outer tips, can be varied. The control design task for constant-speed pitch-regulated machines is to exploit this capability in order to regulate power output whilst minimising the load transients and thereby reducing fatigue damage. The objectives of the SISO control system are discussed fully by Leithead *et al.* (1991a, b, 1992).

Wind turbine power regulation presents a demanding SISO control problem with the plant, actuation system and control objectives all strongly nonlinear. Having catered adequately for the nonlinear plant dynamics (Leithead *et al.* 1991a, 1992, Leith & Leithead 1995), the plant may be considered to be essentially linear but the control objectives remain nonlinear. In this paper, a novel nonlinear control strategy is presented which addresses the nonlinear control objectives. This controller is, in some sense, optimal across the operating envelope rather than at an operating point.

A conceptually simple approach to the design of a nonlinear controller is to construct it by continuously interpolating, in some manner, between the members of a family of linear controllers. Each linear controller might be designed on the basis of a linearisation, at a specified operating point, of the plant. When the controller is adjusted with reference to a slowly varying externally measured quantity (that is, the operating point is parameterised by such a quantity), it is usually referred to as a 'gain-scheduled' controller. However, this term is also widely applied, in a somewhat imprecise manner, to encompass a broad range of systems including those where the scheduling variable varies rapidly and where an internal state of the controller is employed to implicitly schedule the system. These latter systems may be strongly nonlinear and their dynamic characteristics may, in general, bear little relation to that of traditional slowly varying exogenously gain-scheduled systems. In order to emphasise their essentially nonlinear nature, it is proposed, within the context of this paper, that 'interpolated linear controller' is a more appropriate, and conceptually clearer, term with which to denote this broad class of systems. 'Gain-scheduled' is then reserved to describe systems which are sufficiently slowly-varying that, in the context of a particular application, the characteristics of the family of linear controllers are inherited by the interpolated linear controller and so-called frozen-time linear analysis is applicable (trivially, when the rate of variation is zero).

Whilst interpolated linear controllers occur frequently (*e.g.* Astrom & Wittenmark 1989, Hyde & Glover 1990), techniques for the analysis and design of these systems are poorly developed. In a context related to gain-scheduling, Lawrence & Rugh (1993, 1995) propose that a necessary condition for the properties of the members of the family of linear controllers to be inherited by an interpolated linear controller is that the linearisation, at a specific equilibrium operating point, of the nonlinear system corresponds to the associated member of the family of linear controllers. When the parameter variation in an unforced interpolated linear system is sufficiently slow the nonlinear behaviour of the system is weak and linear stability analysis is valid (Desoer 1969). Moreover, robustness is preserved with respect to convolution operator feedback perturbations (Shamma & Athans 1987) and finite-dimensional nonlinear perturbations (under certain conditions, Desoer & Vidyasagar 1975). However, the tests of slowness are often very conservative and may involve quantities for which values are difficult to obtain (Shamma & Athans 1987, 1990). Shamma & Athans (1990) extend their analysis to forced gain-scheduled systems, but their results are confined to two specific arrangements and they observe that evaluation of the sufficiency bounds obtained is impractical. In the forced case, a general result from singular perturbation theory (Hoppensteadt 1966, Khalil & Kokotovic 1991) indicates local stability if the inputs vary sufficiently slowly that the system remains close to a family of equilibrium operating points. However, the local nature of this result restricts its utility. When the members of the linear family of controllers are sufficiently alike, stability of the associated interpolated linear controller is assured (Shahruz & Behtash 1992, Becker *et al.* 1993). The smoothness requirements imposed are, however, very restrictive.

In the present application, the realisation adopted enables the use of an interpolated linear controller in circumstances which are not, *a priori*, warranted by weakness of the nonlinearities. (Wind speed fluctuations are highly stochastic and the operating point of a wind turbine varies rapidly and continuously over the whole operational envelope. Whilst, typically, the bandwidth of the closed-loop system is 3 r/s, the operating point might cover its full range in one or two seconds (Leithead *et al.* 1991a). Consequently, the emphasis is on the nonlinear behaviour and performance of the controlled system). Although it is known that the dynamic characteristics of interpolated linear controllers with integral action depend substantially on the positioning

of the pure integrator relative to the rest of the controller (Leithead *et al.* (1991a), in the context of strongly nonlinear control; Lawrence & Rugh (1993,1995), Kaminer *et al.* (1995) in contexts related to gain-scheduling), the influence of the choice of realisation adopted otherwise appears to have received little consideration.

The paper is organised as follows. Section Two outlines the controller specification. In Sections Three, Four, Five and Six the nonlinear control approach is discussed, including the selection of an appropriate realisation. In Section Seven, results from extensive simulations are used to compare the performance of the nonlinear controller with conventional linear control. Due to lack of space, attention is confined to continuous-time control of a typical 300 kW two-bladed machine with full-span pitch regulation. Similar results are obtained with other configurations of wind turbine (Leith & Leithead 1994a,b). In Section Eight, the conclusions are summarised.

2. Controller Specification

In this paper, controllers are described for a medium-scale wind turbine which is dynamically representative of commercial machines of its class. A block diagram of the linearised wind turbine control model is depicted in figure 1. The open-loop system dynamics, at a wind speed of 12 m/s, are modelled by the transfer function $G(s)$ (see Leithead *et al.* 1991a for details of the nonlinear representation) where

$$G(s) = \frac{1.553 \times 10^{10}(s+4.0)}{(s^7 + 1.073 \times 10^2 s^6 + 5.917 \times 10^3 s^5 + 2.263 \times 10^5 s^4 + 4.393 \times 10^6 s^3 + 3.927 \times 10^7 s^2 + 1.932 \times 10^8 s + 4.423 \times 10^8)}$$

It is important that fair comparisons between controller performance are made. To this end each controller investigated is required to have similar stability margins and to operate within the same actuator restrictions. All the controllers are designed to meet the following requirements :

- (i) Gain margin of at least 10 dB.
- (ii) Phase margin of approximately 60 degrees.
- (iii) Servo pitch acceleration standard deviation no more than approximately 20 deg/s².

The aerodynamic behaviour of wind turbine blades is highly nonlinear and strongly dependent on wind speed. In terms of a linearised plant description, as wind speed increases the gain of the plant increases since the rate of change of aerodynamic torque to pitch angle increases. It is standard practice for wind turbine controllers to include a nonlinear gain to compensate for this variation and make the control task essentially linear (Leith & Leithead 1995, Leithead *et al.* 1991a). Because of their global mutual compensation (Leith & Leithead 1995), these two nonlinearities are ignored in the remainder of this paper. (The dynamics at all wind speeds may now be considered to be the same and modelled by $G(s)$). However, the representation of the aerodynamics is very basic and subject to considerable uncertainty. Consequently, a good gain margin, in conjunction with a good phase margin, is particularly important in order to achieve adequate stability margins. Because of the complexity of the interaction of the rotor with the wind, it is not possible to quantify the uncertainty in the aerodynamic gain but practical experience indicates that 10 dB is an appropriate gain margin. If adequate gain and phase margins are not achieved the system must sometimes destabilise, although not necessarily become unstable, in which case the wind turbine would experience large load fluctuations.

Requirement (iii) represents a practical limitation on the level of activity of the blade servo. Servo pitch acceleration is a measure of the force or torque developed by the actuator and the standard deviation reflects activity over the medium and long term. It should be emphasised that the value of pitch acceleration used is *not* that of the actual turbine blades. Rather, it is a normalised measure which permits valid comparisons to be made between differing designs of actuator. For example, blade pitching systems with different gearing ratios linking the actuator to the blades may be compared in an unbiased manner using this measure. The pitch acceleration of the actual blades will typically have a lower value as a result of the compliance of the blades and linkages together with many other factors. The restriction on actuator activity inherent in (iii) is always necessary to prevent saturation occurring too frequently but there may also be additional hardware-related reasons for its imposition. For the machine considered here, the actuator is an electro-mechanical system and the restriction on servo pitch acceleration is equivalent to a restriction on the servo motor current which is imposed to prevent over-heating. The limit of 20 deg/s² is typical of comparable commercial machines.

There are several implementation issues which need to be considered. The actuator, in addition to requirement (iii), is subject to hard limits on torque, velocity and position and effective anti-wind-up measures are therefore important. There is, also, the requirement to ensure smooth and timely start-up of the controller. (When the wind speed falls below a certain level, rated power cannot be generated and control action is suspended until the wind speed rises again). These issues have a significant impact on performance and are discussed in detail elsewhere (Leith & Leithead 1995, Leithead *et al.* 1991a). It should be noted that the nature of the realisation of the controller is important when addressing the implementation issues and also impacts strongly upon the effectiveness of the compensating nonlinear gain discussed above. The controller realisations adopted in this paper are compatible with the requirements thereby imposed (Leith & Leithead 1995, Leithead *et al.* 1991a).

3. Nonlinear Control

The actuator characteristics, especially the limits on torque, are one of the main restrictions on the performance that can be achieved by a controller. As the wind speed rises, a linear controller places less demand on the actuator since the sensitivity of the aerodynamic torque to pitch changes increases faster than the sensitivity to wind speed changes. Hence, for a controller with fixed open-loop cross-over frequency, whilst the actuator may be worked to its full capability at low wind speed, it is not used as fully at higher wind speeds. However, it is at these higher wind speeds that loads are greatest and therefore controller performance is most critical. Parametric studies (Rogers & Leithead 1993, 1994 and Leithead and Rogers 1993) indicate that there is an advantage in using this spare actuator capacity as the wind speed rises and that there exists an optimum level of activity for the controller at each wind speed. Whether, at any particular wind speed, the resulting optimum cross-over frequency can be achieved in practice depends on the capabilities of the actuator.

The optimum, as measured by the standard deviation of the power transients (see figure 2) exists due to the action of two competing factors. As wind speed rises, for a fixed controller the standard deviation of the power also rises due to the increased level of turbulence. It is therefore attractive to increase the controller activity by raising the open-loop cross-over frequency, giving improved disturbance rejection. However, the wind spectrum differs from that experienced at a static point (see, for example, Leithead *et al.* 1991a). In particular, the wind experienced by a wind turbine contains large amounts of energy at frequencies nP , where n is the number of blades or an integer multiple thereof, and P is the rotational speed of the rotor. Since it is necessary to protect the actuator by causing the open-loop transmittance to roll-off, whilst maintaining adequate gain and phase margins, there is an inevitable tendency for the sensitivity transfer function to increase the intensity of the nP peaks as the cross-over frequency is increased.

The requirement is to design a controller which operates as near as possible to its optimal level of activity in all wind speeds, subject to actuator constraints. A complication is the lack of a direct measurement of wind speed. Indeed there is no such thing as 'the windspeed' experienced by a wind turbine, since the rotor experiences a spatially and temporally distributed wind field. Simple scheduling is therefore not appropriate and the wind speed must be inferred from the plant dynamics via the pitch demand. If the controller is operating correctly, the demanded pitch angle is a good indicator of wind speed. (This approach is widely used to vary the previously noted nonlinear gain, which essentially linearises the plant by compensating for variations in the aerodynamic torque sensitivity). Employing an internal state of the system, such as the pitch demand, to implicitly change the controller as wind speed varies must be treated with some caution, however, since it introduces additional nonlinear feedback loops, thereby changing the plant dynamics. The design task is to develop a continuously varying controller which induces the appropriate closed-loop dynamics at any wind speed, despite the presence of these feedback loops. The resulting controller is nonlinear.

A family of linear controllers is designed for various wind speeds using classical loop-shaping design techniques. Taking some care to minimise the differences between them, the family of controller transfer functions obtained is :

$$g(u) = \frac{(s^2+7.59s+68.06) (s+1.7)(s+1.8)(s^2+3s+416.16)(s^2+2s+104.04)(s^2+7.243s+38.637)2209}{(s^2+a(u)s+b(u)) s(s+0.3)(s+3.7)(s^2+8s+416.16)(s^2+11s+104.04)(s+100)(s+30)(s^2+65.8s+2209)}$$

where $a(u)=-0.033047u^2 + 0.75064u + 3.3749$, $b(u)= 2.6002u + 58.040$, $g(u)=(0.13779u + 0.29784)$, and u is the nominal pitch angle, in degrees, demanded by the controller at the equilibrium operating points. It can be seen that these controller transfer functions are the same except for a varying gain and a pair of varying

poles. The Bode plot of the open-loop transfer function of the system with the member of this family of controllers for 12 m/s wind speed is shown in figure 3. The family of controllers exhibits low frequency shaping to improve disturbance rejection, high frequency roll-off to reduce actuator activity, and notches at 2P and 4P to reduce actuator activity and reduce the enhancement of the loads induced by these spectral peaks. The gain and phase margins of the transfer functions for specific members of the family are given in the following table :

u (deg)	gain margin (dB)	phase margin (deg)	cross-over freq. (r/s)
3.84 (12 m/s)	13.74	55.23	1.36
11.14 (16 m/s)	10.03	55.89	2.51
16.21 (20 m/s)	10.00	55.62	2.85
20.59 (24 m/s)	10.79	55.64	3.25

As may be seen from figure 2, the optimum cross-over frequencies to minimise the standard deviation of the power output are approximately 1.5 r/s, 2.25 r/s and 4 r/s at 12 m/s, 16 m/s and 23m/s respectively for this configuration of wind turbine (Rogers & Leithead 1993, 1994, Leithead & Rogers 1993). While at 24 m/s the optimum cross-over frequency of around 4 r/s is not achieved due to the physical limitations of the actuator, the minima is broad and the cross-over frequency of 3.25 r/s is near optimal. The gain margin of the 12 m/s controller is rather higher than 10 dB. Since there is always a trade-off between performance and robustness, the controller does not achieve the best performance possible at low wind speeds. This choice of controller is necessary, however, if the variation between the transfer functions of the controllers is to be restricted to the values of a, b and g.

The controller is split into two main blocks as shown in figure 4 to cater for the situation when a negative pitch angle is demanded, i.e. when the wind speed has fallen below the level at which rated power of 300 kW can be generated. In this situation the controller is switched out of operation . Owing to the presence of low frequency dynamics within the controller, transients may occur for a substantial period of time when the controller is switched back in again as the wind speed rises. To combat the transients, a minor loop is introduced within the controller which is activated during below rated operation so that the controller is continuously operating and thereby smooth switching achieved. This technique, including the partitioning of the controller into inner and outer blocks, is discussed in detail in Leith & Leithead (1995) and Leithead *et al.* (1991a, 1992). The controller partitioning in the present case is as follows:

$$\text{Inner Block } 4.5g(u) \frac{(s+1.7)(s+1.8)(s^2+7.59s+68.06)}{s(s+0.3)(s+3.7)(s^2+a(u)s+b(u))}$$

$$\text{Outer Block } 0.222 \frac{(s^2+7.243s+38.637)(s^2+2s+104.04) (s^2+3s+416.16)}{(s+100)(s+30)(s^2+11s+104.04)(s^2+65.8s+2209) (s^2+8s+416.16)}$$

A nonlinear controller is obtained by interpolating continuously between the members of the family of linear controllers as pitch demand varies. Upper and lower bounds are placed on a, b and g. When u is less than 3.84 degrees (corresponding to 12 m/s wind speed), a, b and g are held at their 3.84 degree values. Similarly, when u is greater than 20.59 degrees (24 m/s wind speed), a, b and g are held at their 20.59 degree values. The nonlinearities are confined to the inner block of the controller.

It is known (see, for example, Leithead *et al.* 1991a, 1992) that the dynamic behaviour of a nonlinear controller can strongly depend upon the realisation adopted. In particular, for controllers with integral action, the position of the pure integrator is important (Leithead *et al.* 1991a, 1992). Perhaps an obvious choice of realisation for the inner block is to group the nonlinear elements together and place them after all the linear dynamic terms (including the pure integrator term). Alternatively, the nonlinear elements might be positioned after the main linear dynamics but immediately before the pure integrator. The performance, as indicated by generated power, is depicted in figure 5a with the nonlinear elements positioned both after the pure integrator and before. (The precise realisation for the latter is that of figure 6a and the realisation for the former is the same except for repositioning of the pure integrator). A considerable difference in performance is evident. Of course, when the nonlinear nature of the controller is sufficiently weak, the

realisation adopted is immaterial. Hence, the comparison acts as a simple test of the strength of nonlinearity. The extent of the difference in performance in figure 5a, between the pure integrator being positioned before the nonlinear elements and after, indicates that, in the present case, the nonlinearity is not *a priori* weak. Clearly, the influence of the choice of realisation is substantial and must be considered with some care.

It has been proposed by Leith & Leithead (1994c) that a nonlinear controller constructed by interpolating between linear controllers should satisfy a local linear equivalence condition; that is, the linearisation, at any operating point, of the nonlinear controller should correspond to the associated member of the family of linear controllers. In contrast, Lawrence & Rugh (1993,1995) restrict local linear equivalence to only the equilibrium operating points; that is, operating points for which the plant and controller states and the scheduling variables have constant values. Exploiting the particular characteristics of the class of equilibrium operating points, an algebraic condition is derived specifically for local linear equivalence at the equilibrium operating points. Lawrence & Rugh (1993,1995) observe that, for controllers with integral action, local linear equivalence at equilibrium operating points is achieved by adopting a realisation in which the pure integrator term is placed after the other dynamic elements. Since the realisation depicted in figure 6a meets this requirement, it attains local linear equivalence at the equilibrium operating points. In addition, the realisation of figure 6a has the desirable property that, at an equilibrium operating point, variations in the nonlinear terms, a, b and g which are unrelated to the input to the controller are rejected by the controller; that is, the system will remain in equilibrium regardless of spurious fluctuations in these terms. Both these properties of the controller are a direct consequence of the signals, upon which the nonlinear terms act, having zero value in equilibrium owing to the position of the pure integrator.

However, figure 6a does not represent a unique choice of representation and many satisfy the local linear equivalence condition at equilibrium operating points; for example, alternative realisations are depicted in figures 6b and 6c. (Without undue difficulty, when implementing the controller with the realisation of figure 6c, it can be reformulated to accommodate the improper transfer function). Lawrence & Rugh (1993, 1995) do not distinguish between different realisations that satisfy the local linear equivalence condition at equilibrium operating points. However, they are not equivalent. Figure 5b compares the power outputs, in response to a sequence of moderate gusts, for the controller realisations of figures 6a and 6c. It is clear that the behaviour exhibited by the controllers is substantially different despite both displaying local linear equivalence at the equilibrium operating points.

Furthermore, although realisations satisfying the local linear equivalence condition of Lawrence & Rugh (1993, 1995) are not distinguishable at the equilibrium operating points, the neighbourhoods of the equilibrium operating points, within which they are dynamically similar to the associated linear systems, can vary substantially. Consider the realisations of figures 6a and 6b. For constant values of a, b and g (that is, the linear time-invariant case), the realisations of figures 6a and 6b are equivalent and typical of implementations that might be employed for linear systems. For time-varying values, the dynamic behaviour of the second order nonlinear element in figure 6b is described by the differential equation

$$\ddot{x}_3 + a(u)\dot{x}_3 + b(u)x_3 = x_1 \quad (1)$$

To clarify the analysis, the time-invariant zeroes of the second order nonlinear element are, without loss of generality, neglected. Locally to an equilibrium operating point at which the nominal value of u is u_0 ,

$$u = u_0 + \delta u \quad (2a)$$

$$x_1 = 0 + \delta x_1; \quad x_3 = 0 + \delta x_3; \quad \dot{x}_3 = 0 + \delta \dot{x}_3; \quad \ddot{x}_3 = 0 + \delta \ddot{x}_3 \quad (2b)$$

and equation (1) has the linearisation

$$\delta \ddot{x}_3 + a(u_0)\delta \dot{x}_3 + b(u_0)\delta x_3 \approx \delta x_1 \quad (3)$$

From (3), it is clear that the local linear equivalence condition is satisfied at the equilibrium operating points. The error, ϵ , in approximating (1), locally to the equilibrium operating point, by (3) is

$$\epsilon = (a(u) - a(u_0))\delta \dot{x}_3 + (b(u) - b(u_0))\delta x_3 \quad (4)$$

Since $a(\bullet)$ and $b(\bullet)$ are continuous and non-zero for all possible values of u, it follows that ϵ can be made arbitrarily small for δu sufficiently small (and δx_3 and its derivative finite); that is, the linearisation accurately describes the dynamic behaviour of (1) in an arbitrarily large neighbourhood in state-space about the equilibrium point provided δu is sufficiently small. Now, consider the realisation of figure 6a. The differential equation (1) is superseded by

$$\ddot{x}_3 + a(u)\dot{x}_3 + b(u)x_3 + \frac{da}{du}\dot{u}x_3 = x_1 \quad (5)$$

(again neglecting zeroes). Locally to an equilibrium operating point, the differential equation (5) might again be approximated linearly by (3) and the local linear equivalence condition is again satisfied at the equilibrium operating points. The error, ξ , in approximating (4), locally to the equilibrium point, by (3) is

$$\xi = \left(a(u) - a(u_0) \right) \delta x_3 + \left(b(u) - b(u_0) \right) \delta x_3 + \frac{da}{du}(u) \delta u \delta x_3 \quad (6)$$

In general, δu can be arbitrarily large independently of the magnitude of δu and so, unless δx_3 is confined to an infinitesimally small neighbourhood about the origin, ξ may be large even if δu is small. Although it is unlikely that δu is unduly large for ideally deterministic systems, to which Lawrence & Rugh (1993, 1995) is restricted, this possibility is not so unlikely for stochastic systems where, for example, high frequency measurement noise might be present. In practice, therefore, the neighbourhoods of the equilibrium operating points, within which (1) and (5) are dynamically similar to (3), may be quite different. Indeed, (5) may exhibit substantially different dynamic behaviour from (1) and from that indicated by its linearisation local to an equilibrium operating point, even when δu is small and the states of the system are rather close to their equilibrium values. The better realisation is apparently (1).

From the foregoing discussion it is evident that simply requiring local linear equivalence at the equilibrium points provides an inadequate basis for the choice of realisation for interpolated linear controllers. Dynamic behaviour far from the equilibrium points cannot be neglected. In unsteady operating conditions, substantial prolonged perturbations from the equilibrium operating point are experienced in many applications. For example, in the wind turbine case, the wind turbulence does not consist solely of small wind speed fluctuations about some mean value. Large, rapid fluctuations in wind speed and power output are common, in particular gusts; that is, steady increases or decreases in the wind speed which persist for relatively long periods. Hence, it is insufficient to consider only the dynamic behaviour of the system close to the equilibrium operating points; conditions which are far from equilibrium cannot be neglected. The stronger criterion of Leith & Leithead (1994c) is required.

4. Realisation of the Nonlinear Controller

4.1 Extended Local Linear Equivalence

A SISO interpolated linear system is described by the nonlinear differential equation

$$\dot{\mathbf{x}} = \mathbf{F}(\mathbf{x}, r, \rho); \quad y = H(\mathbf{x}, r, \rho) \quad (7)$$

where $\mathbf{F}(\bullet, \bullet, \bullet)$, $H(\bullet, \bullet, \bullet)$ are differentiable, r denotes the input to the system, y the output and ρ is a continuous scalar function of (\mathbf{x}, r) corresponding to the scheduling variable. The set of equilibrium operating points consists of those points, (\mathbf{x}_0, r_0) , for which $\mathbf{F}(\mathbf{x}_0, r_0, \rho_0)$ is zero, where ρ_0 denotes $\rho(\mathbf{x}_0, r_0)$. Let $\Phi: \mathcal{R}^n \times \mathcal{R}$ denote the space $\{(\mathbf{x}, r)\}$. The set of equilibrium operating points forms a locus in Φ and the response of the system to the general time-varying input, $r(t)$, is depicted by a trajectory in Φ . Satisfying local linear equivalence at the equilibrium operating points as proposed by Lawrence & Rugh (1993, 1995) ensures that the interpolated linear system exhibits similar behaviour to the appropriate linear system near a specific equilibrium operating point only if (\mathbf{x}, r) (and so also $\rho(\mathbf{x}, r)$) remains within a sufficiently small (perhaps vanishingly small) neighbourhood of that operating point. The size of the neighbourhood about each operating point depends on the strength of nonlinearity of the system. Outwith each neighbourhood the interpolated linear system can exhibit very different characteristics from the local linearisation. The situation is illustrated by figure 7a for a SISO first-order system: the neighbourhoods, depicted about specific equilibrium operating points, notionally indicate the respective regions within which linearisation is valid.

In general, for linearisation to provide a valid indication of the dynamic behaviour near an equilibrium point requires

- (i) sufficiently small variations in the scheduling variable, ρ
- (ii) every state to remain within a small neighbourhood of the specific equilibrium operating point
- (iii) sufficiently small variations in the input, r .

Since the nonlinear character of an interpolated linear system is embodied in the scheduling variable, ρ , it is reasonable to expect restrictions on the allowable behaviour of ρ for linear analysis to apply. In contrast, the latter two conditions represent very strong restrictions which do not seem to be *a priori* necessary yet limit the analysis to small (perhaps vanishingly small) neighbourhoods, in the space Φ , of the equilibrium operating points (requiring, implicitly, every system state to be, in some sense, slowly-varying).

Behaviour at the equilibrium points alone provides little indication, in general, of the utility of a realisation for an interpolated linear system, the behaviour of the realisation at every operating point in Φ must, instead, be considered. Leith & Leithead (1994c) proposed that local linear equivalence should be

required at all operating points, whether equilibria or not. This condition subsumes that of equivalence at the equilibrium operating points alone and corresponds to the natural requirement that the linearisation about every point in Φ for which ρ equals ρ_o should be identical to the member, specified by ρ_o , of the family of linear controllers. Since ρ is scalar, ρ equals ρ_o upon a surface of dimension $(n-1)$ in Φ . Moreover, for the linearisation of the nonlinear system to be parameterised purely by ρ it follows that $\nabla_x \rho$ and $\nabla_r \rho$ are functions of ρ alone and so are constant over the surface in Φ upon which ρ equals ρ_o . Hence, the normal to that surface is identical at every point on the surface and the surface must, therefore, be a hyperplane. In figure 7b, the shaded region notionally indicates the neighbourhood of linear equivalence about a specific hyperplane. Local linear equivalence, in this extended sense, thus, ensures that the family of linear systems indicate the local dynamic behaviour at every point in Φ , as required, rather than only in a small region close to the locus of equilibrium operating points. In addition, it ensures that linear analysis is applicable to any trajectory for which ρ is constant; that is, trajectories lying wholly on a hyperplane of constant ρ . Hence, for the dynamic behaviour of the realisation to be globally appropriate only the scheduling variable, ρ , is subject to a restriction on its rate of variation, which surely represents the minimum constraint. In contrast to the extended local linear equivalence condition, the local linear equivalence condition of Lawrence & Rugh (1993, 1995), as noted above, requires that every element of (\mathbf{x}, \mathbf{r}) remains within a small neighbourhood of the equilibrium point which indirectly imposes a constraint on the rate of variation of the states. In general, the resulting restriction on $\dot{\rho}$ is stricter than under the extended local linear equivalence condition.

It follows immediately from the extended local linear equivalence condition that the nonlinear components of the implemented interpolated linear system must be purely functions of ρ ; that is, the nonlinear system has the form

$$\dot{\mathbf{x}} = \mathbf{A}\mathbf{x} + \mathbf{B}\mathbf{r} + \mathbf{f}(\rho) \quad (8a)$$

$$y = \mathbf{C}\mathbf{x} + \mathbf{D}\mathbf{r} + h(\rho) \quad (8b)$$

where \mathbf{A} , \mathbf{B} , \mathbf{C} , \mathbf{D} are constant matrices, $\mathbf{f}(\rho)$ and $h(\rho)$ are differentiable functions and $\nabla_x \rho$ and $\nabla_r \rho$ are functions of ρ alone. Consequently, the hyperplanes of constant ρ in Φ do not intersect; that is, the hyperplanes, and so their normals, must be parallel for all ρ . Hence, it may be assumed, without loss of generality, that $(\nabla_x \rho, \nabla_r \rho)$ is a constant vector and ρ is a linear combination of the states and the input. Assuming that the point (\mathbf{x}, \mathbf{r}) lies in a sufficiently small neighbourhood of the hyperplane containing the equilibrium point $(\mathbf{x}_o, \mathbf{r}_o)$, then

$$\mathbf{f}(\rho) \approx \mathbf{f}(\rho_o) + \mathbf{f}'(\rho_o)(\rho - \rho_o) = \mathbf{f}(\rho_o) + \mathbf{f}'(\rho_o)(\nabla_x \rho \Delta \mathbf{x} + \nabla_r \rho \Delta \mathbf{r})$$

$$h(\rho) \approx h(\rho_o) + h'(\rho_o)(\rho - \rho_o) = h(\rho_o) + h'(\rho_o)(\nabla_x \rho \Delta \mathbf{x} + \nabla_r \rho \Delta \mathbf{r})$$

and the nonlinear system (8) has the linearisation

$$\Delta \dot{\mathbf{x}} \approx \{\mathbf{A} + \mathbf{f}'(\rho_o) \nabla_x \rho\} \Delta \mathbf{x} + \{\mathbf{B} + \mathbf{f}'(\rho_o) \nabla_r \rho\} \Delta \mathbf{r} \quad (9a)$$

$$\Delta y \approx \{\mathbf{C} + h'(\rho_o) \nabla_x \rho\} \Delta \mathbf{x} + \{\mathbf{D} + h'(\rho_o) \nabla_r \rho\} \Delta \mathbf{r} \quad (9b)$$

where $\mathbf{x} = \mathbf{x}_o + \Delta \mathbf{x}$; $\mathbf{r} = \mathbf{r}_o + \Delta \mathbf{r}$; $y = y_o + \Delta y$ and $y_o = \mathbf{C}\mathbf{x}_o + \mathbf{D}\mathbf{r}_o + h(\rho_o)$. Note, $\Delta \mathbf{x}$ and $\Delta \mathbf{r}$ need not be small. Unfortunately, the utility of (9) is hindered by the states being different from those in the nonlinear system (8) and varying with the operating point. Moreover, (8) and (9) have different forms and the relationship between them is not transparent. These issues are resolved by reformulating (9) as

$$\dot{\mathbf{x}} \approx -\{\mathbf{A} + \mathbf{f}'(\rho_o) \nabla_x \rho\} \mathbf{x}_o - \{\mathbf{B} + \mathbf{f}'(\rho_o) \nabla_r \rho\} \mathbf{r}_o + \{\mathbf{A} + \mathbf{f}'(\rho_o) \nabla_x \rho\} \mathbf{x} + \{\mathbf{B} + \mathbf{f}'(\rho_o) \nabla_r \rho\} \mathbf{r} \quad (10a)$$

$$y \approx y_o - \{\mathbf{C} + h'(\rho_o) \nabla_x \rho\} \mathbf{x}_o - \{\mathbf{D} + h'(\rho_o) \nabla_r \rho\} \mathbf{r}_o + \{\mathbf{C} + h'(\rho_o) \nabla_x \rho\} \mathbf{x} + \{\mathbf{D} + h'(\rho_o) \nabla_r \rho\} \mathbf{r} \quad (10b)$$

and differentiating (10) to obtain

$$\dot{\mathbf{w}} \approx \{\mathbf{A} + \mathbf{f}'(\rho_o) \nabla_x \rho\} \mathbf{w} + \{\mathbf{B} + \mathbf{f}'(\rho_o) \nabla_r \rho\} \mathbf{r} \quad (11a)$$

$$\dot{y} \approx \{\mathbf{C} + h'(\rho_o) \nabla_x \rho\} \mathbf{w} + \{\mathbf{D} + h'(\rho_o) \nabla_r \rho\} \mathbf{r} \quad (11b)$$

where \mathbf{w} equals \mathbf{x} . When the right-hand side of (8a) is invertible, so that \mathbf{x} may be expressed as a function of \mathbf{w} and \mathbf{r} , then restricting the domain of \mathbf{w} restricts the range of \mathbf{x} and (11) is an alternative linearisation of (8). In addition, an alternative representation

$$\dot{\mathbf{w}} = \{\mathbf{A} + \mathbf{f}'(\rho(\mathbf{w}, \mathbf{r})) \nabla_x \rho\} \mathbf{w} + \{\mathbf{B} + \mathbf{f}'(\rho(\mathbf{w}, \mathbf{r})) \nabla_r \rho\} \mathbf{r} \quad (12a)$$

$$\dot{y} = \{\mathbf{C} + h'(\rho(\mathbf{w}, \mathbf{r})) \nabla_x \rho\} \mathbf{w} + \{\mathbf{D} + h'(\rho(\mathbf{w}, \mathbf{r})) \nabla_r \rho\} \mathbf{r} \quad (12b)$$

of the nonlinear dynamics is obtained by differentiating (8). The relationship between the linearisation (11) and the nonlinear system (12) is direct; indeed, (11) is simply the frozen-time form of (12). The dependence upon \mathbf{r} in (11) and (12) is purely a consequence of the states selected and may be removed by an appropriate state transformation (see section 4.2).

The foregoing analysis assumes that a suitable scheduling variable, ρ , has been selected. Shamma & Athans (1990), in accordance with common guidelines, indicate that this variable should reflect the plant nonlinearity and be relatively slowly varying.

4.2 Realisations with Extended Local Linear Equivalence

It is necessary to determine whether requiring the controller to be a member of the class of interpolated linear systems which satisfy the extended local linear equivalence condition for a suitable choice of realisation is restrictive.

Consider the nonlinear system

$$\begin{bmatrix} \dot{x}_1 \\ \dot{x}_2 \\ \vdots \\ \dot{x}_{n-1} \\ \dot{x}_n \end{bmatrix} = \begin{bmatrix} -A_1(x_1 + b_1 r) + x_2 + b_2 r \\ -A_2(x_1 + b_1 r) + x_3 + b_3 r \\ \vdots \\ -A_{n-1}(x_1 + b_1 r) + x_n + b_n r \\ -A_n(x_1 + b_1 r) + r \end{bmatrix}; \quad y = G(x_1 + b_1 r) \quad (13)$$

for some functions $G(\bullet)$ and $A_n(\bullet)$. The system (13) has the form required by (8) and, therefore, meets the the extended local linear equivalence condition. When $A_n(\bullet)$ is invertible, (13) can be reformulated as in (12). In addition, when $G(\bullet)$ is invertible the scheduling variable can be replaced by y . With these invertibility conditions, an alternative representation, for which the associated family of linear systems consists of the frozen-time linearisations, is

$$\begin{bmatrix} \dot{w}_1 \\ \dot{w}_2 \\ \vdots \\ \dot{w}_{n-1} \\ \dot{w}_n \\ \dot{y} \end{bmatrix} = \begin{bmatrix} -a_1(y) (w_1 + b_1 \dot{r}) + w_2 + b_2 \dot{r} \\ -a_2(y) (w_1 + b_1 \dot{r}) + w_3 + b_3 \dot{r} \\ \vdots \\ -a_{n-1}(y) (w_1 + b_1 \dot{r}) + w_n + b_n \dot{r} \\ -a_n(y) (w_1 + b_1 \dot{r}) + \dot{r} \\ g(y) (w_1 + b_1 \dot{r}) \end{bmatrix} \quad (14)$$

with $\mathbf{w} = \mathbf{x}$, $a_i(y) = A_i'(G^{-1}(y))$, $i=1..n$, and $g(y) = G'(G^{-1}(y))$. The requirement on (13) that $G(\bullet)$ and $A_n(\bullet)$ are invertible becomes a requirement on (14) that $g(y)$ and $a_n(y)$ have fixed signs. Any realisation related to (13) and (14) by a non-singular linear time-invariant state transformation clearly also displays extended local linear equivalence. The nonlinear systems, (13) and (14), are the realisations depicted in figures 8 and 9, respectively. At every point in state-space where x_1 has the value x_{10} , and so y has the value $y_0 = G(x_{10})$, the linearisations of figure 8 or 9 have the transfer function

$$Y(s) = g(y_0) \frac{b_1 s^n + b_2 s^{n-1} + \dots + b_n s + 1}{s^n + a_1(y_0) s^{n-1} + \dots + a_{n-1}(y_0) s + a_n(y_0)} R(s) \quad (15)$$

where $Y(s)$ and $R(s)$ are the Laplace transforms of $y(t)$ and $r(t)$, respectively.

For a specific interpolated linear controller parameterised by y , for which the transfer functions of the corresponding family of linear controllers are known and conform to (15), $G(\bullet)$ and $A_i(\bullet)$, $i=1..n$, are determined from

$$A_i(\rho) = \int_0^\rho a_i(G(s)) ds; \quad G(y) = \int_0^y g(s) ds \quad (16a)$$

with suitable boundary conditions; for example,

$$A_i(0) = 0 = G(0) \quad (16b)$$

ensures that, in equilibrium, the output, y , is zero for r zero. Whilst the realisation of figure 8 is directly applicable to controllers without integral action, the pure integrator in the realisation of figure 9 is an essential element of that realisation and cannot be omitted. Controllers without integral action can, nonetheless, be accomodated, in almost all cases when $G(\bullet)$ and $A_n(\bullet)$ are invertible, within the realisation of figure 9 by reformulating the controllers to act on r rather than \dot{r} in order to introduce integral action. The realisation of figure 9 has the distinct advantages of being directly related to the members of the family of linear controllers from which the interpolated linear controller is constructed.

Adoption of the realisation of figures 8 or 9 ensures that the extended local linear equivalence condition is satisfied for the class of interpolated linear SISO controllers for which the system poles are scheduled by an internal state but the zero dynamics are fixed. Moreover, with the penalty of a non-minimal realisation, it is straightforward to show that a change in the magnitude and phase of a transfer function arising from a modification of the location of a zero may equivalently be obtained by an appropriate modification of the location of a pole. Hence, realisations of the form in figures 8 and 9, with varying poles, can be employed to implement interpolated linear SISO designs with varying zeroes. Indeed, this may be achieved directly, by selecting the family of linear controllers, upon which the interpolated linear controller is based, such that every member has identical zeroes; that is, during synthesis, without loss of generality, the variation between members is confined to the overall gain and the poles.

It is self-evident that the realisations considered here can be applied to any interpolated linear controller scheduled on an internal state; in particular, the controller output which is usually the most appropriate since it has a tendency to be the most slowly varying. The realisations can also be applied to those scheduled on a plant state, x , by employing the arrangement depicted in figure 10. P_1 is the operator relating x to the plant input and it is assumed that the inverse operator P_1^{-1} , or a suitable realisable approximation, exists. To illustrate scheduling on a plant state, consider the following situation. In the nonlinear controller of section 3, the nonlinear terms are functions of the pitch demand output of the controller. Although the wind speed is better indicated by the actual pitch angle of the blades, the pitch demand is a satisfactory alternative because the actuator has a high bandwidth (around 20 r/s) relative to that of the controlled system. However, were the actuator to be much slower, for example, with transfer function $0.3/(s+0.3)$, then the controller should be scheduled on the blade pitch angle; that is, a plant state. The required arrangement is that depicted in figure 10, with P_1 equal to $0.3/(s+0.3)$. Simulation studies undertaken to estimate the performances of this arrangement and the original realisation of figure 6a modified by scheduling on its actual pitch angle rather than pitch demand (so no longer exhibiting extended local linear equivalence) indicate that the power outputs differ by more than 30 kW.

5. Realisation of Wind Turbine Nonlinear Controller

In section 4, it is shown that extended local linear equivalence is ensured for a wide class of interpolated linear SISO systems by adopting an appropriate realisation. The implications for the wind turbine nonlinear controller of section 3 need to be evaluated.

In section 3, three realisations of the wind turbine nonlinear controller are considered; namely, those of figures 6a and 6b, which are equivalent to the nonlinear differential equations (1) and (5), respectively, and that of figure 6c. All three exhibit local linear equivalence at the equilibrium operating points. However, even locally, as discussed in section 3, the dynamic behaviour of the realisations can be considerably different since the control signals have substantial high frequency component due to disturbances at nP (and hence δu in (6) cannot *a priori* be expected to be relatively small). Since (4) is not dependent on δu , the realisation of figure 6b is initially deemed preferable. However, it is immediately evident that the realisation depicted in figure 6a corresponds to that of figure 9, for a second order system, and satisfies the extended local linear equivalence condition while the realisation of figure 6b does not. (It should be noted that both $b(\bullet)$ and $g(\bullet)$ have fixed sign and the controller has integral action, as required). Surprisingly, therefore, it must be concluded that the realisation of figure 6a and not figure 6b is the most appropriate. The relationship of the realisation of figure 6a to the other two realisations is discussed below.

Firstly, the relationship of the realisation of figure 6b to that of figure 6a is considered. The dynamic behaviour of these realisations are closely related: they can be made dynamically equivalent, for example, by introducing an additional term in (1) such that x_1 is replaced by $x_1 - \dot{a}(u)x_3$; that is, replacing $b(u)$ by $b(u) - \dot{a}(u)$ in figure 6b. The introduction of terms involving derivatives of the nonlinear elements in (1) is somewhat counter-intuitive and emphasises the need for an analytic basis for the choice of realisation. Only when the nonlinear behaviour is sufficiently weak that the term $\dot{a}(u)x_3$ is negligible are the realisations in figures 6a and 6b equivalent. Simulation studies encompassing a wide range of wind conditions indicate that, for these two realisations, the power output typically only differs by about 1 kW, in comparison with a standard deviation of the power about the rated value of approximately 40 kW. Hence, in the context of this particular application, the feedback term, $\dot{a}(u)x_3$, may indeed be neglected and the second order network is weakly nonlinear in the sense that its dynamic behaviour is insensitive to the realisation adopted.

Secondly, the relationship of the realisation of figure 6c to that of figure 6a is considered. Simulation studies indicate that the dynamic behaviour is essentially unchanged when the low frequency pole (of

frequency 0.3 r/s) in the realisation of figure 6a is repositioned after the nonlinear second order network but immediately before the nonlinear gain, $g(u)$, thereby confirming the weakly nonlinear nature of the second order network. However, it is clear, see figure 5b, that substantially different dynamic behaviour is exhibited when the low frequency pole is positioned after the gain, $g(u)$ to obtain the realisation of figure 6c. The gain, $g(u)$, cannot, therefore, be considered to be *a priori* weakly nonlinear in the sense that its dynamic behaviour does not depend on the realisation adopted. With the low frequency pole positioned immediately after the nonlinear gain, $g(u)$; that is, the realisation of figure 6c (neglecting, without loss of generality, the above mentioned pole-zero pair),

$$\ddot{u} + 0.3\dot{u} = g(u) x_4 \quad (17)$$

where x_4 is the output of the nonlinear second order network. With the low frequency pole positioned immediately before the nonlinear gain,

$$\ddot{u} + 0.3\dot{u} - \frac{\dot{g}}{g}(u)\dot{u} = g(u) x_4 \quad (18)$$

The dynamic relationships (17) and (18) only differ by the term $\frac{\dot{g}}{g}(u)\dot{u}$. If the realisation of figure 6c is

modified by adding the feedback signal $\frac{\dot{g}}{g^2}(u)\dot{u}$ to x_4 , then these two realisations become equivalent. The

term $\frac{\dot{g}}{g^2}(u)\dot{u}$ has fixed sign (since $\frac{dg}{du}$ has fixed sign) and it introduces a positive bias, evident in figure

5b, of up to 50 kW in the power during gusts. Hence, in the context of this particular application, the feedback term, $\frac{\dot{g}}{g^2}(u)\dot{u}$, cannot be neglected and the nonlinear gain is not *a priori* weak.

The realisation of figure 6a, which satisfies the extended local linear equivalence condition strictly, regardless of the strength of the nonlinearities, is adopted for the inner block of the nonlinear wind turbine controller (Leith & Leithead 1994c[†]).

6. Dynamic Analysis of Nonlinear Controller

Although the extended linear equivalence criterion introduced above does not guarantee that the performance requirements are met by the interpolated linear controller, it does provide additional guidance for the design of this type of controller. As usual, the dynamic behaviour must be confirmed by analysis and/or simulation. In particular, the non-local stability and robustness properties of the nonlinear controller, which depend on the choice of realisation, must be similar to those of the linear controllers. The nonlinear control strategy involves implicit scheduling on an internal controller state which is not, *prima facie*, slowly varying. The stability and robustness of such a controller can be investigated using a variety of methods. Two approaches to stability and robustness analysis are considered here, namely: (i) Small Gain theorem, (ii) rate of controller variation. Whilst the analytic tools are more conservative than in those available for the analysis of linear systems the success of the choice of realisation of the nonlinear controller, in causing it to inherit the properties of the family of linear controllers, can be expected to be reflected in the results.

(i) The Small Gain theorem (see for example Desoer & Vidyasagar 1975) is one of the most useful tools for the analysis of nonlinear systems, particularly where the system contains important linear elements, as in the present case. In order to use a small gain approach in the current application, the system is reformulated as in figure 11. In figure 11, N_o is a linear approximation to the nonlinear second-order network, N ; C_o is the outer block of the controller plus the time-invariant part of the inner block; g_L is a constant gain approximating the nonlinear controller gain, g . Δ accommodates the nonlinear behaviour of both the second-order network, N , and the control gain, g .

Employing the Small Gain theorem, it is determined that the closed-loop system is stable for $|g_L + \Delta|$ in the ranges (0.00, 5.55) and (3.33, 11.49). Δ may be decomposed into a component Δ_N associated with the nonlinear behaviour of the second-order network, N , and a component Δ_g associated with the nonlinear behaviour of the control gain g . These components may be isolated using the following approximate method. N is obtained by interpolating between linear time-invariant operators N_L . With the 24 m/s case as N_o , the

[†] The figure in Leith & Leithead 1994c illustrating the realisation is, unfortunately, incorrect; the realisation adopted was in fact that of figure 6a in the present paper.

ratios between the magnitudes of $N_L'(s)$ and of $N_o'(s)$ are easily calculated (where N_L' denotes the Laplace transform of N_L , etc). Taking the peak value of these ratios as an estimate of $1+|\Delta_N|$, bounds on $|\Delta_g|$ are found from the bounds on $|\Delta|$. The permitted ranges for $|\Delta_g|$ are (0.00, 5.30) and (3.18,10.97). Given that the actual values of the gain g lie between 1.50 and 3.46, the first range for $|\Delta_g|$ indicates that the system should be stable for the nominal plant and controller whilst the second range indicates that stability is maintained when the variation in the inner block gain is increased by a factor of 3.17, i.e. there is a gain margin of at least 10.02dB. ■

(ii) For a nonlinear system composed of a linear dynamic element and a single time-varying gain, a result due to Desoer & Vidyasagar (1975) provides a sufficient condition on the gain to ensure that the system exhibits weakly nonlinear behaviour and admits linear analysis. Weak nonlinearity in this sense may result from both sufficiently slow variation of the gain and/or variation which is sufficiently small in magnitude. Specifically, the closed-loop system is stable if,

$$\sup_{t \in [0, \infty)} \int_0^t |H_t(t-\tau) \{g(t)-g(\tau)\}| d\tau < 1$$

where $g(\bullet)$ is the varying gain, and $H_t(\bullet)$ is the impulse response of the linear time invariant closed-loop system obtained with g set constant to the value it attains at time t . It is assumed that this impulse response is bounded; that is, the time-invariant system is stable. The result requires that $g(\bullet)$ remains sufficiently constant during the 'memory time' of $H_t(\bullet)$ (the period when H_t differs appreciably from zero). It is satisfied if $g(\bullet)$ is slowly varying over time, or if the variation in the magnitude of $g(\bullet)$ is sufficiently small (even if this variation is rapid), or for some suitable combination of these characteristics.

In order to apply this result to the present case, it is necessary to assume that the nonlinear behaviour exhibited by the second-order network, N , is sufficiently weak that it admits linear analysis. The assumption is supported by the results of section 4.4 and by the following argument. The linear transfer functions in the family, which forms the basis for N , only differ significantly from one another at frequencies above 5 r/s, and have unity gain at lower frequency. Linear analysis should, therefore, certainly apply at low frequencies. N is varied with pitch demand which has little frequency content above 2-3 r/s. Hence, with respect to frequencies above 5 r/s, N appears to be slowly varying, as required. If the maximum magnitude of the rate of change of $g(\bullet)$ is α , then we have that

$$|g(\tau) - g(t)| \leq \alpha |\tau - t|$$

Numerically evaluating the integral reveals that values of α up to 1.12 are permissible. An estimate of the actual value of α can be obtained from

$$\alpha = dg/dt = (dg/du) (du/dt)$$

where u is the pitch demand signal used to vary the controller. It is known that $dg/du \leq 0.14$ and it is determined from simulations that $du/dt \leq 2$ deg/s. Hence, $dg/dt \leq 0.28$ and the system is stable. Furthermore, this result suggests that the nonlinear behaviour can be considered to be sufficiently weak that stability may be predicted by linear analysis. Given the rapid variation in pitch demand in absolute terms, whereby the full controller range could be covered in one or two seconds, this is a somewhat unexpected conclusion. ■

Whilst neither of the stability results presented above are conclusive, it is believed that they are based on reasonable assumptions and they appear to be consistent with one another and with the properties of the family of linear systems. That the latter is the case is an indication, supported by the lack of conservativeness of the results, that the choice of realisation successfully enables the interpolated linear controller to be applied when, *a priori*, not warranted by weakness of the nonlinearity.

In extensive simulations carried out with the controller for various wind conditions it is confirmed that the controller performs as intended. Specifically, even in very turbulent conditions (up to 20% turbulence intensity) the performance of the nonlinear controller closely agrees with that of the member of the family of linear controllers for the corresponding mean wind speed. In further simulations in which the gain of the controller increased, a gain margin of around 10.9 dB is observed at wind speeds around 24 m/s. At lower wind speeds the gain margin appears to be greater. This behaviour is in surprisingly good agreement with

the gain margins predicted by the analysis carried out when designing the controller. By introducing a first order all-pass network with a non-minimum phase zero, the effect of phase changes may also be investigated. In simulations the system is marginally stable for a non-minimum phase zero at $s=-5$ r/s, corresponding to a 62 degree phase lag at 3 r/s, the approximate controller cross-over frequency .

7. Performance Assessment & Comparison

The performance of the nonlinear control strategy is investigated using a well validated simulation methodology. For comparison, a conventional linear controller designed to meet the same specifications is also considered:

Linear Controller (see for example Leithead *et al.* 1991a, 1992):

$$871.229 \frac{(s+1.6)^2(s^2+7.243s+38.637)(s^2+1.5s+104.04)(s^2+6s+416.16)}{s(s+0.3)(s+3.7)(s+20)(s+50)(s^2+11s+104.04)(s^2+10s+416.16)(s^2+65.8s+2209)}$$

(gain margin 10 dB, phase margin 56.14 degrees, cross-over frequency 1.826 r/s). This controller is similar to previous controllers used with a commercial two-bladed design of wind turbine (Leithead & Agius 1991, Bossanyi *et al.* 1992).

Assessment of the performance follows the well-validated approach of Leithead & Agius (1991) and Bossanyi *et al.* (1992). Simulation runs are performed with each specific controller over a range of wind speeds and turbulence levels. Four mean wind speeds of 12, 16, 20 and 24 m/s were used at three nominal turbulence levels of 10, 15 and 20 %. Each simulation run is of 260 seconds duration, giving 4 one minute periods of data per run, after discarding the initial 20 seconds to allow the system to settle down, and 48 one minute periods over all the runs. (A data sampling rate of 50 Hz is used). The nominal turbulence level only applies over a long time period and the range of turbulence levels for the one minute samples is 6 - 26 %. While turbulence in the range 8 - 18 % corresponds to the moderate wind conditions noted Leithead & Agius (1991) and Bossanyi *et al.* (1992), results for slightly more turbulent conditions with intensity in the range 13 - 26 % are presented in this paper. For each one minute sample, within the specified turbulence range, the maximum power was plotted against the mean wind speed over that sample. A linear fit to this data then provides an indication of the trend in maximum power with wind speed. Moreover, if the standard deviation of the residues of the maxima about the linear fit is determined, then the power maxima experienced under normal operating conditions are unlikely to exceed the linear fit by more than three times the standard deviation. Empirical investigations (Leithead & Agius 1991, Bossanyi *et al.* 1992) have shown that despite the small number of data points used, this approach is nevertheless a good indicator of the comparative performance between controllers.

Before considering results based on the above one minute binning approach, an indication of the relative performance of the controllers is obtained by comparing the probability distributions of the power time histories for these controllers. These are given in figure 12 for typical power time histories at a mean wind speed of 24 m/s, 20% turbulence intensity. A large reduction in the time spent at high power levels is evident with the nonlinear controller. For example, the percentage of time that the power level exceeds 450 kW for the nonlinear controller is 0.64 % compared with 4.02 % for conventional linear control. Similar results are obtained at other wind speeds and turbulence levels (Leith & Leithead 1994c).

The equations of linear fits to the power maxima, from the one minute samples with turbulence in the range 13-26 %, are given in the table below. The plot in figure 13 shows the three standard deviation line associated with each fit. As noted, this line provides an indication of the maximum power likely to be encountered during normal operation. Once again, the performance achieved with the nonlinear controller is a substantial improvement over that with linear control.

Controller	Fit	Standard Deviation
linear	8.49w+280.05	20.02
nonlinear	5.11w+330.49	14.52

The power maxima for the nonlinear controller increase at only around two-thirds the rate of those for linear control. The reduced rate of increase of the maxima in combination with much lower standard deviations of

the residues, corresponding to tighter bunching of the maxima, represents a significant overall reduction in the peak power excursions likely to be experienced and a consequent reduction in drive-train load transients.

The pitch acceleration standard deviations for the one minute samples are shown in figure 14. The linear controller works the actuator hardest at low wind speeds but the actuator activity falls rapidly as the wind speed rises due to the increase in the sensitivity of the aerodynamic torque to pitch changes. In contrast, the standard deviation for the nonlinear controller remains roughly constant as wind speed rises, exploiting the extra actuator capacity available at higher wind speed as intended.

More detailed results are contained in Leith & Leithead (1994a, b) together with results for a three-bladed machine.

8. Conclusion

In the control design task for pitch-regulated constant-speed wind turbines, the plant, actuation system and control objectives are all strongly nonlinear. Having catered adequately for the nonlinear plant dynamics (Leithead *et al.* 1991a, 1992, Leith & Leithead 1995), the plant may be considered to be essentially linear but the control objectives remain nonlinear. Improvement in the controller performance can still be achieved by adjusting the controller as the operating point changes. Wind speed fluctuations are highly stochastic and the operating point of a wind turbine varies rapidly and continuously over the whole operational envelope. Consequently, the emphasis is on the nonlinear behaviour and performance when considering control strategies which are adjusted as the operating point changes. An interpolated linear control strategy is presented in which the control algorithm continuously changes with the operating point in such a way that the controller is instantaneously always the most appropriate for the inferred wind speed. The resulting control strategy with integral action may, in some sense, be considered to be optimised across the operating envelope rather than at an operating point. From the results of extensive tests using a well validated simulation methodology, the performance of a typical two-bladed configuration of wind turbine is compared for the nonlinear controller and a conventional linear controller. The simulations confirm that the nonlinear controller performs as intended. Nonlinear control is found to reduce both the peak power and the time spent at high power levels in comparison to linear control, with a consequent reduction in drive-train loads. The improvement is obtained by exploiting the actuator capability left unused at higher wind speeds by linear time-invariant controllers and is cheap in the sense that to achieve the same improvement by means of linear control, were it possible within practical constraints, would require much greater and expensive actuator capability than is typically available. The improvement in performance, in comparison to conventional linear control, is substantial.

The nature of the realisation of the nonlinear controller is demonstrated to be crucial in attaining the required performance. (Much greater care is required for this aspect of the controller design than for the synthesis of the linear algorithm embedded within it). Of course, when the nonlinear characteristics are sufficiently weak the dynamic behaviour exhibited is insensitive to the realisation adopted; the influence of the choice of realisation upon performance is therefore employed as a novel measure, which is direct and straightforward to apply, of the strength of nonlinear behaviour. With regard to previous, somewhat scarce, results in the literature concerning the choice of realisation of interpolated linear controllers it is noted that local linear equivalence condition at the equilibrium operating points (Lawrence & Rugh 1993, 1995) is of little utility and that, even locally, controller realisations satisfying this condition may exhibit substantially different dynamic behaviour. An extended local linear equivalence condition is, therefore, introduced which is of general application and subsumes the previous condition. This condition ensures that at every operating point the linearisation of the nonlinear controller matches the appropriate member of the family of linear controllers upon which the design is based. The extended local linear equivalence condition does not require that the system be *a priori* slowly varying and is not confined to the equilibrium operating points. Indeed, equivalence holds equally at equilibrium operating points and at unsteady operating points far from equilibrium. Realisations which display this property are derived for a wide class of SISO interpolated linear systems (those scheduled upon an internal plant or controller signal). With regard to the wind turbine application, the interpolated linear controller satisfying the extended local linear equivalence condition causes a large reduction (50 kW) in the power peaks in comparison to realisations which only satisfy local linear equivalence about the equilibrium operating points but not the extended criterion. This reduction is similar to that achieved by appropriately realised nonlinear control in comparison to linear control; thereby illustrating the importance of adopting an appropriate realisation.

Acknowledgements

The EPSRC, DTI (formerly D.En) and ETSU, by whose permission this paper is published, are gratefully acknowledged for supporting the work presented.

References

- ASTROM, K.J., WITTENMARK, B., 1989, *Adaptive Control* (New York, Addison-Wesley).
- ATHERTON, DP, 1982, *Nonlinear Control Engineering* (New York: Van Nostrand Reinhold).
- BOSSANYI, E.A., SMITH, G.J., LEITHEAD, W.E., AGIUS, P., 1992, Design and Testing of a Classical Controller for the MS-3. Wind Turbine Final Report E/5A/CON/6033/2184, Energy Technology Support Unit, Harwell, Oxfordshire OX11 0RA, U.K.
- DESOER, C.A., 1969, Slowly Varying System $dx/dt=A(t)x$. *IEEE Transactions on Automatic Control*, **14**, 780-781.
- DESOER, C.A., VIDYASAGAR, M., 1975, *Feedback Systems: Input-Output Properties* (London : Academic Press).
- HOPPENSTEADT, F.C., 1966, Singular Perturbations on the Infinite Interval. *Transactions of the American Mathematical Society*, **123**, 521-535.
- HYDE, R.A., GLOVER, K., 1993, The Application of Scheduled H_{∞} Controllers to a VSTOL Aircraft. *IEEE Transactions on Automatic Control*, **38**, 1021-1039.
- KAMINER, I., PASCOAL, A., KHARGONEKAR, P., COLEMAN, E., 1995, ρ A Velocity Algorithm for the Implementation of Gain-Scheduled Controllers. *Automatica*, **31**, 1185-1191.
- KHALIL, H.K., KOKOTOVIC, P.V., 1991, On Stability Properties of Nonlinear Systems with Slowly Varying Inputs. *IEEE Transactions on Automatic Control*, **36**, 229.
- LAWRENCE, D.A., RUGH, W.J., 1993, Gain Scheduling Dynamic Linear Controllers for a Nonlinear Plant. *Proceedings of the 32nd Conference on Decision and Control*, San Antonio.
- LAWRENCE, D.A., RUGH, W.J., 1995, Gain Scheduling Dynamic Linear Controllers for a Nonlinear Plant. *Automatica*, **31**, 381-390.
- LEITH, D.J., LEITHEAD, W.E., 1994a, Comparison of Various Control Strategies for a Two-Bladed Wind Turbine. *Proceedings of the British Wind Energy Association Conference*, Stirling.
- LEITH, D.J., LEITHEAD, W.E., 1994b, Benefits of Optimising the Controller with Windspeed for a Constant Speed HAWT. *Proceedings of the European Wind Energy Conference*, Greece.
- LEITH, D.J., LEITHEAD, W.E., 1994c, Application of Nonlinear Control to a HAWT. *Proceedings of the 3rd IEEE Conference on Control Applications*, Glasgow.
- LEITH, D.J., LEITHEAD, W.E., 1995b, An Investigation of the Benefits of Nonlinear Control for Pitch-Regulated Wind Turbines. Report under DTI Agreement No. ETSU W/42/00348/00/00, Industrial Control Centre, Department of Electronic & Electrical Engineering, University of Strathclyde, Glasgow.
- LEITHEAD, W.E., AGIUS, P., 1991, Application of Classical Control to the WEG MS3 Wind Turbine. Report ICU/342, Industrial Control Centre, Department of Electronic & Electrical Engineering, University of Strathclyde, Glasgow.
- LEITHEAD, W.E., DE LA SALLE, S.A., REARDON, D.L., GRIMBLE, M.J., 1991a, Wind Turbine Control Systems Modelling and Design Phase I and II. Department of Trade & Industry Report No. ETSU WN 5108.
- LEITHEAD, W.E., DE LA SALLE, S.A., REARDON, D., 1991b, Role and Objectives of Control for Wind Turbines. *Proceedings of the Institution of Electrical Engineers Pt C*, **138**, 135-148.
- LEITHEAD, W.E., DE LA SALLE, S.A., REARDON, D., 1992, Classical Control of Active Pitch Regulation of Constant Speed HAWTs. *International Journal of Control*, **55**, 845-876.
- LEITHEAD, W.E., ROGERS, M.C.M., 1993, A Comparison of the Performance of Constant Speed HAWT's. *Renewable Energy - Clean Power 2001*, London, IEE Conference Publication No. 385.
- ROGERS, M.C.M., LEITHEAD, W.E., 1994, The Dependence of Control Systems Performance on the Wind Turbine Configuration. Report prepared for AEA Technology, University of Strathclyde.
- ROGERS, M.C.M., LEITHEAD, W.E., 1993, Relationship of the Controllability of Power/Torque Fluctuations in the Drive-Train to the Wind Turbine Configuration. *Proceedings of the 15th British Wind Energy Association Conference*, York.
- SHAHRUZ, S.M., BEHTASH, S., 1992, Design of Controllers for Linear Parameter-Varying Systems by the Gain Scheduling Technique. *J. Mathematical Analysis & Applications*, **168**, 195-217.
- SHAMMA, J.S., ATHANS, M., 1987, Stability and Robustness of Slowly Time-Varying Linear Systems. *Proceedings of the 26th Conference on Decision and Control*, Los Angeles.

SHAMMA, J.S., ATHANS, M., 1990, Analysis of Gain Scheduled Control for Nonlinear Plants. *IEEE Transactions on Automatic Control*, **35**, 898-907.

Figure 1 Linearised control model.

dQ/dp is sensitivity of aerodynamic torque, Q , to changes in pitch, p .
 dQ/dV is sensitivity of aerodynamic torque, Q , to wind speed, V .

Figure 2 - Predicted variance of power output vs open-loop cross-over frequency and wind speed (Leithead & Rogers 1993).

Figure 3 Bode plot of open-loop transfer function with 12 m/s member of family of controllers.

Figure 4 Controller structure.

Figure 5a Comparison of power output for nonlinear gain positioned before and after integrator.

Figure 5b Comparison of power output for the realisations depicted in figures 5a and 5b.

Figure 6 Realisation of inner block of nonlinear controller.

Figure 7a Illustration of local linear equivalence neighbourhoods about constant operating points.

Figure 7b Illustration of extended local linear equivalence neighbourhoods.

Figure 8 Realisation satisfying extended local linear equivalence for varying poles.

Figure 9 Equivalent realisation satisfying extended local linear equivalence for varying poles.

Figure 10 Arrangement for scheduling upon a plant state, x .

Figure 11 Reformulation used for Small Gain theorem analysis of nonlinear controller.

Figure 12 Probability density function of power at 24 m/s, 20% turbulence intensity.

Figure 13 Three standard deviation lines for fits to power maxima.

Figure 14 Pitch acceleration standard deviation.

Figure 1

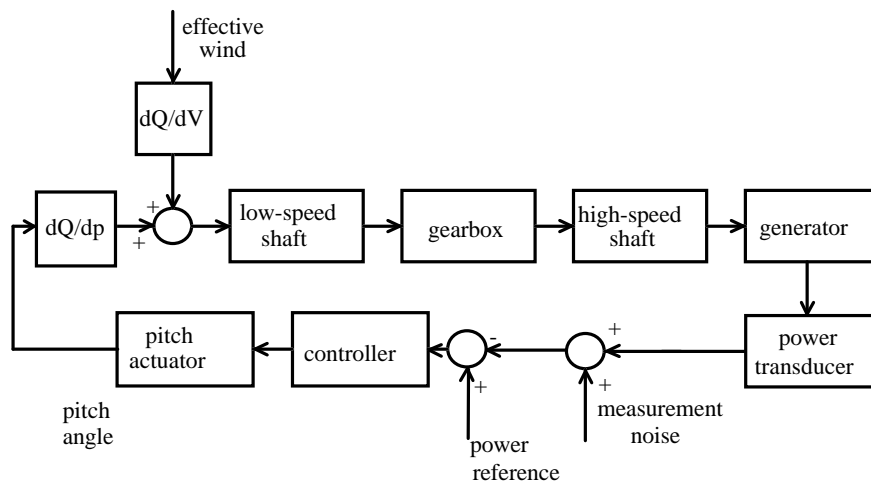


Figure 2

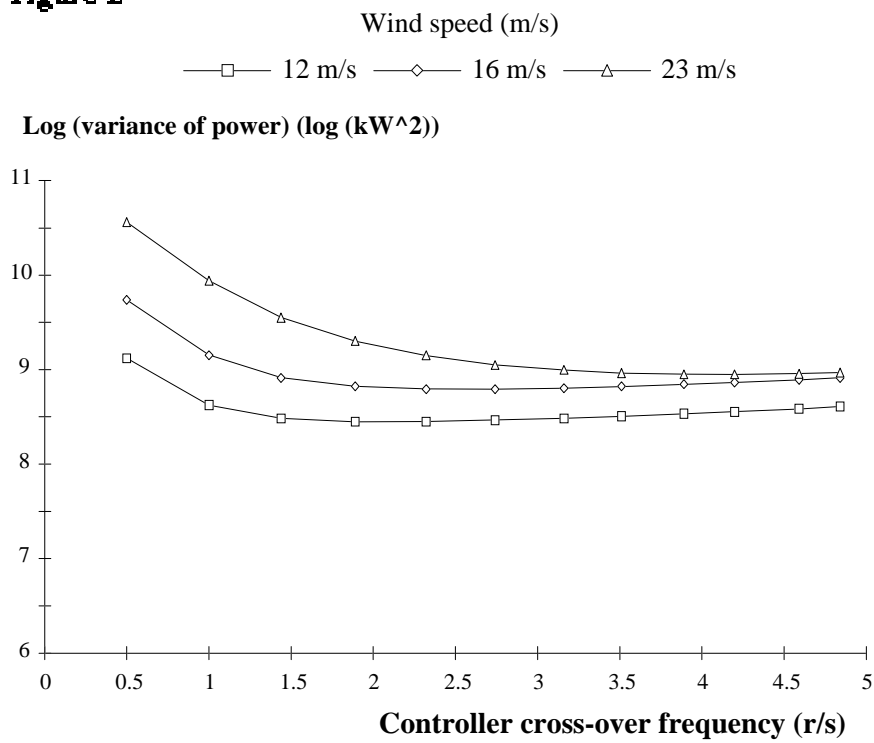


Figure 3

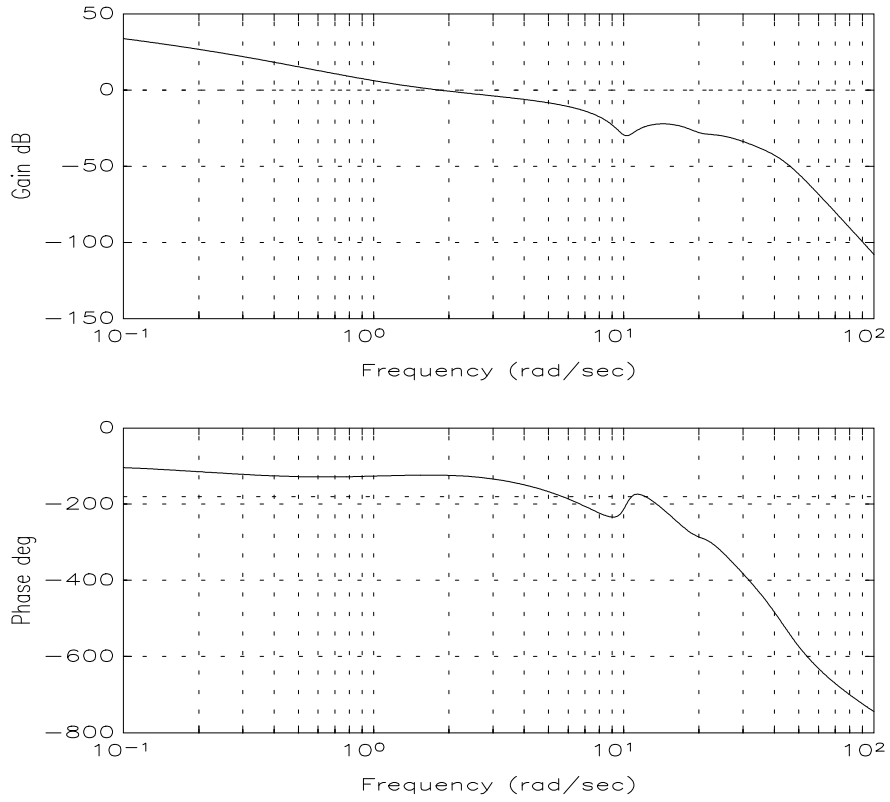


Figure 4

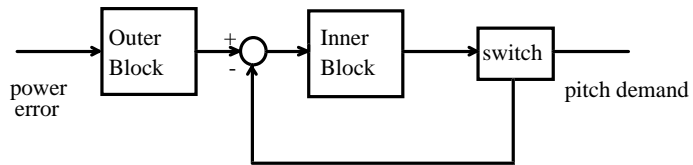


Figure 5a

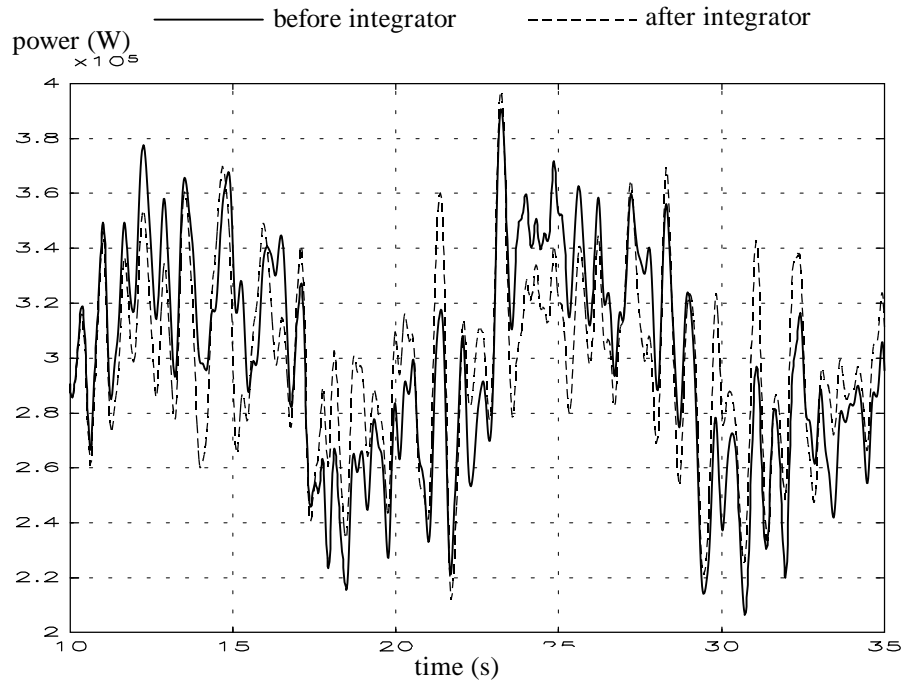


Figure 5b

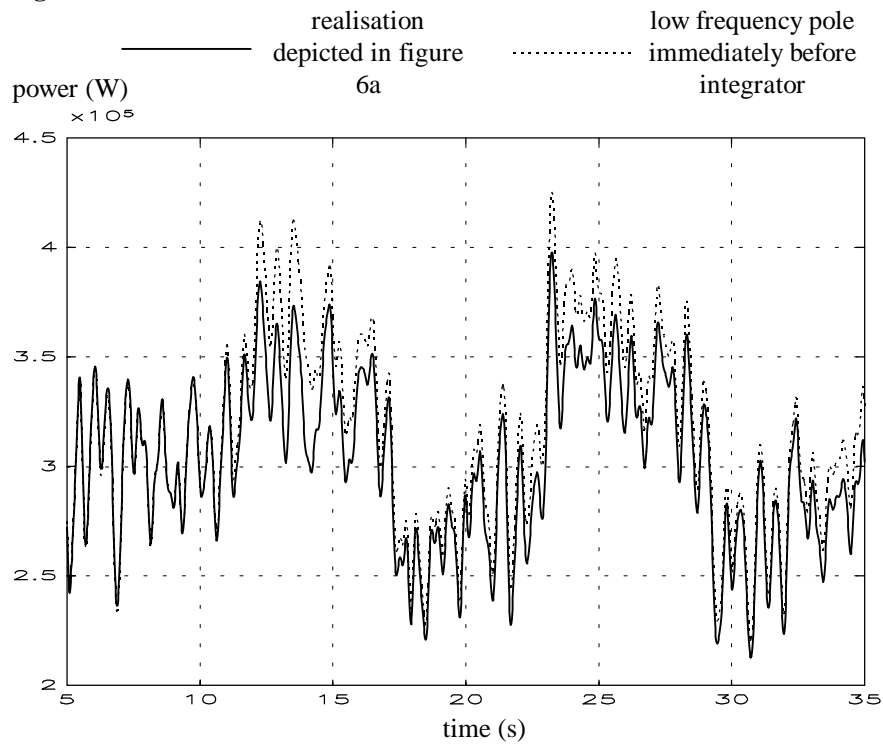


Figure 6a

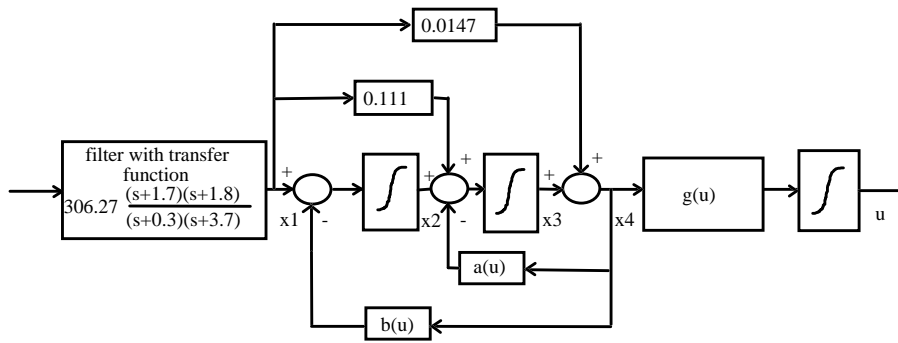


Figure 6b

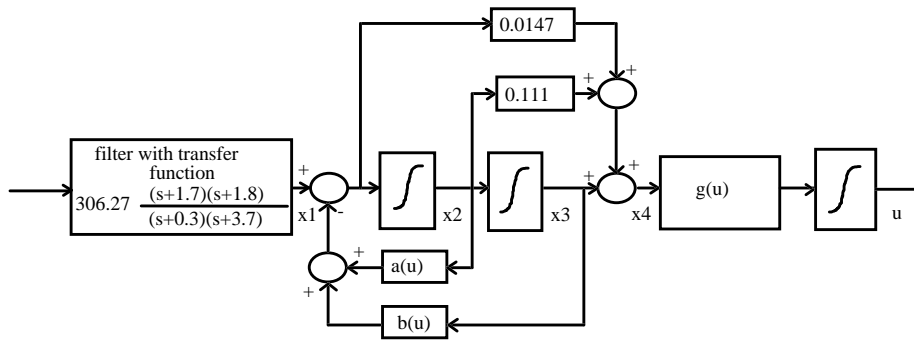


Figure 6c

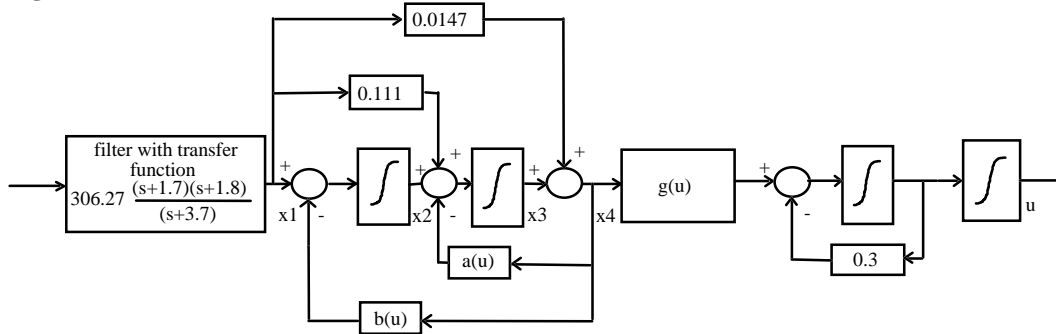


Figure 7a

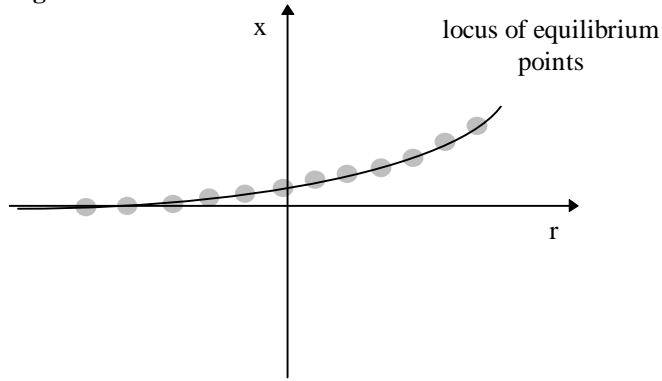


Figure 7b

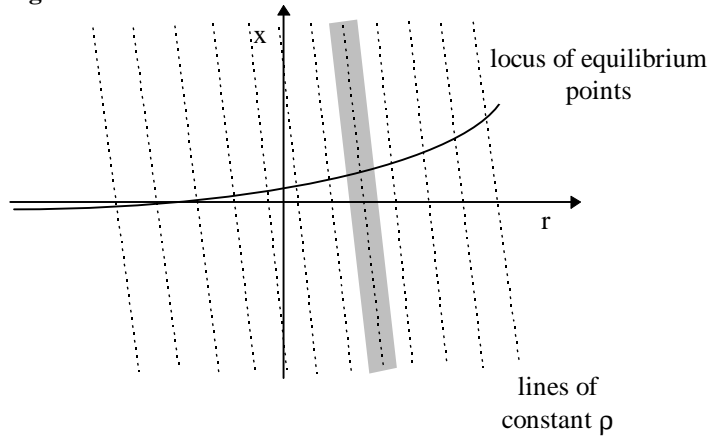


Figure 8

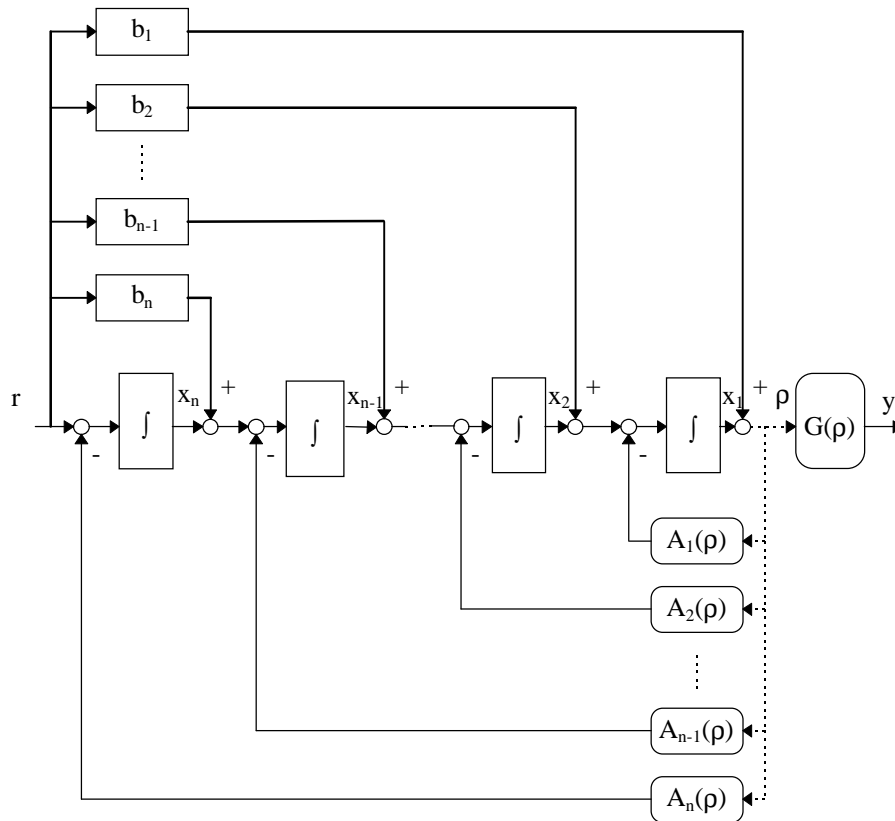


Figure 9

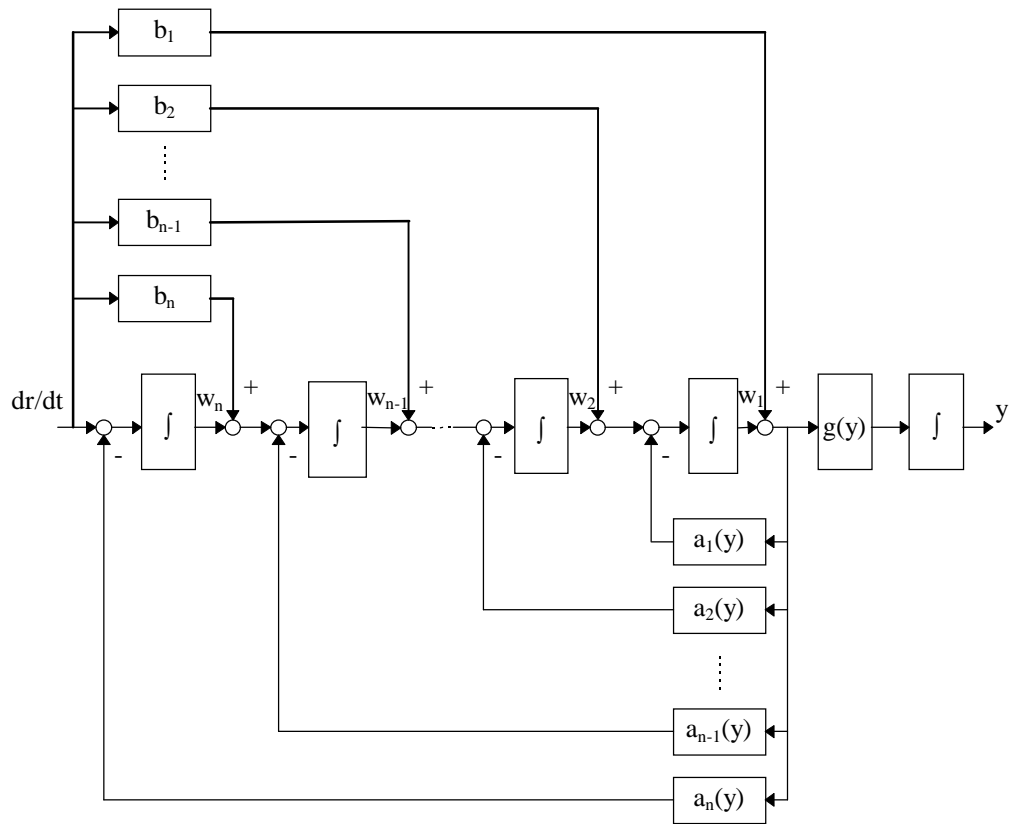


Figure 10

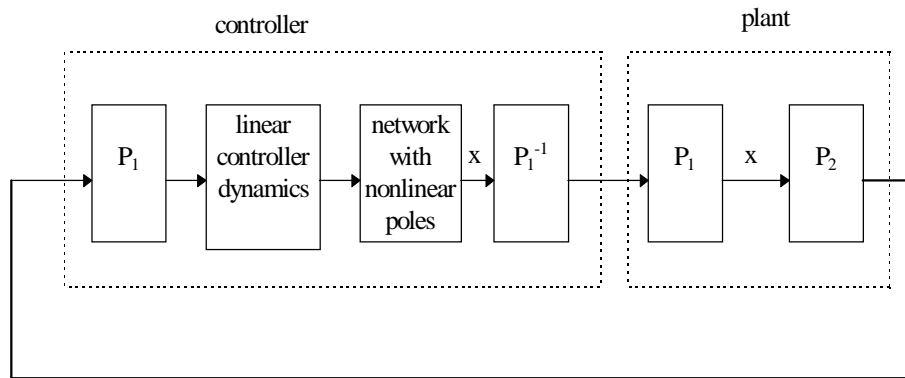


Figure 11

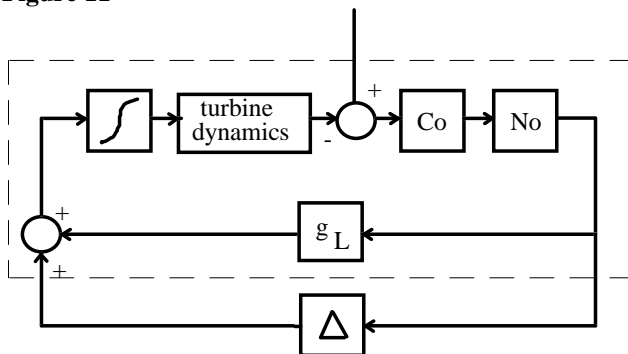


Figure 12

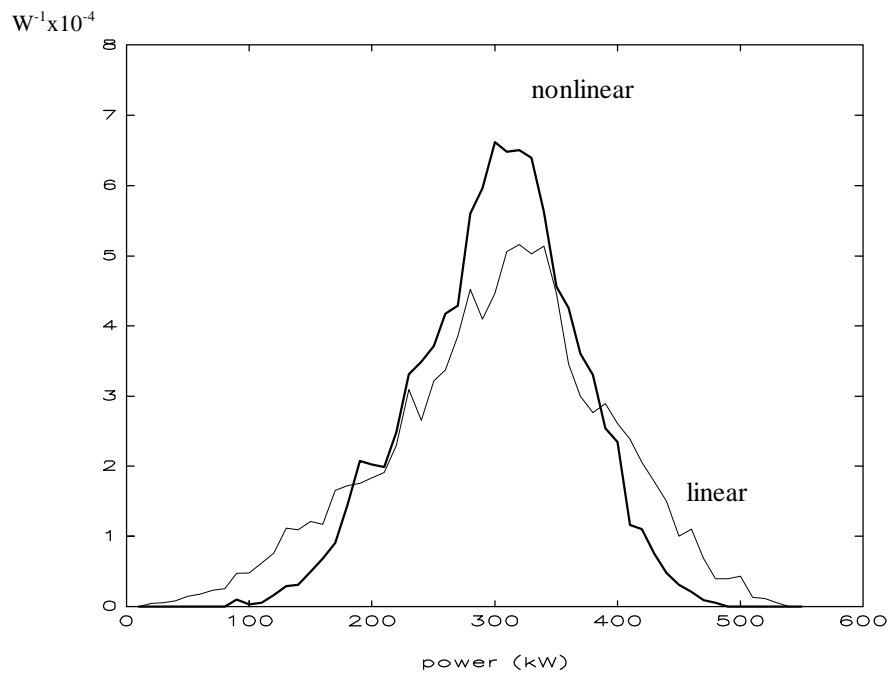


Figure 13

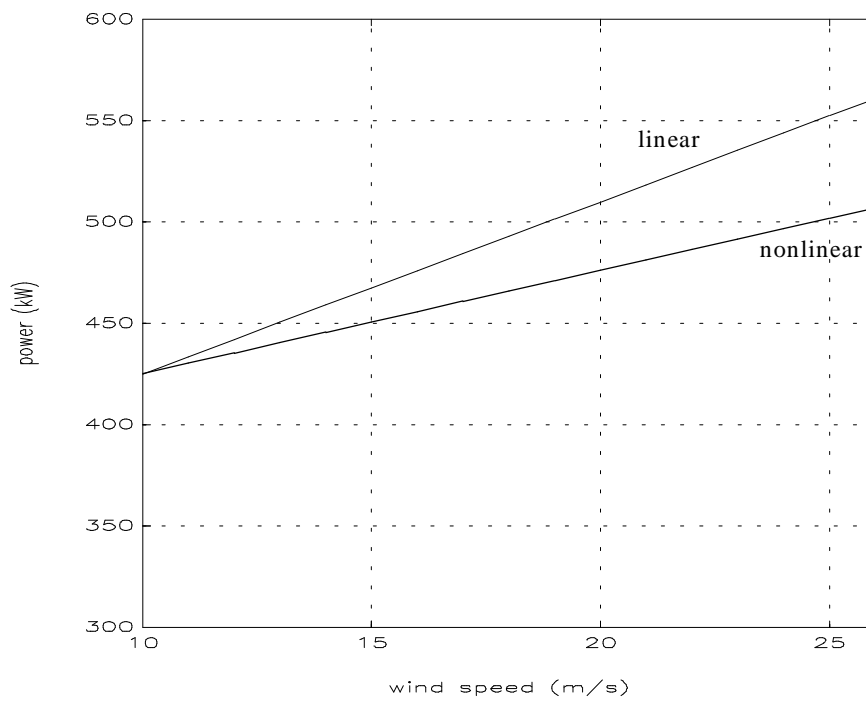


Figure 14

